The local adsorption geometry of CO and NH3 on NiO (1 0 0) determined by scanned-energy mode photoelectron diffraction

ARTICLE *in* SURFACE SCIENCE · FEBRUARY 2002

Impact Factor: 1.93 · DOI: 10.1016/S0039-6028(01)01957-4

9 AUTHORS, INCLUDING:

Jon Tobias Hoeft
GlobalFoundries Inc.
44 PUBLICATIONS **1,086** CITATIONS
SEE PROFILE

Martin Polcik
Beckman Coulter Inc.
89 PUBLICATIONS **1,747** CITATIONS
SEE PROFILE

D. Phillip Woodruff
The University of Warwick
525 PUBLICATIONS **12,812** CITATIONS
SEE PROFILE

C. L. A. Lamont
University of Huddersfield
47 PUBLICATIONS **926** CITATIONS
SEE PROFILE

ELSEVIER

Surface Science 499 (2002) 1–14

SURFACE SCIENCE

www.elsevier.com/locate/susc

The local adsorption geometry of CO and NH_3 on NiO(1 0 0) determined by scanned-energy mode photoelectron diffraction

M. Kittel [a], J.T. Hoeft [a], S. Bao [a], M. Polcik [a], R.L. Toomes [b], J.-H. Kang [b], D.P. Woodruff [a,b,*], M. Pascal [c], C.L.A. Lamont [c]

[a] *Fritz-Haber-Institut der Max-Planck-Gesellschaft, Faradayweg 4-6, D14195 Berlin, Germany*
[b] *Department of Physics, University of Warwick, Coventry CV4 7AL, UK*
[c] *Department of Chemical and Biological Sciences, Centre for Applied Catalysis, University of Huddersfield, Queensgate, Huddersfield HD1 3DH, UK*

Received 28 September 2001; accepted for publication 6 December 2001

Abstract

The local adsorption structures of CO and NH_3 on NiO(1 0 0) have been determined by C 1s and N 1s scanned-energy mode photoelectron diffraction. CO adsorbs atop Ni surface atoms through the C atom in an essentially perpendicular geometry (tilt angle $12 \pm 12°$) with a C–Ni nearest-neighbour distance of 2.07 ± 0.02 Å. NH_3 also adsorbs atop Ni surface atoms with a N–Ni distance of 2.06 ± 0.02 Å. These bondlengths are only very slightly longer than the comparable values for adsorption on metallic Ni surfaces. By contrast theoretical values obtained from total energy calculations, which exist for CO adsorption on NiO(1 0 0) (2.46 Å and 2.86 Å) are very much longer than the experimental value. Similar discrepancies exist for the N–Ni nearest-neighbour bondlength for NO adsorbed on NiO(1 0 0). Combined with the published measurements of the desorption energies, which also exceed the calculated bonding energies, these results indicate a significant failure of current theoretical treatments to provide an effective description of molecular adsorbate bonding on NiO(1 0 0).

Keywords: Photoelectron diffraction; Chemisorption; Surface structure, morphology, roughness, and topography; Nickel oxides; Carbon monoxide; Ammonia; Single crystal epitaxy

1. Introduction

Metal oxide surfaces are widely recognised as being important in the context of heterogeneous catalysis, either as active catalysts in their own right or as supports of metal particles. Despite this, they have, at least until the last few years, been far less extensively studied than metal surfaces using ultra-high vacuum surface science

* Corresponding author. Address: Department of Physics, University of Warwick, Coventry CV4 7AL, UK. Tel.: +44-1203-523378; fax: +44-1203-692016.
E-mail address: d.p.woodruff@warwick.ac.uk (D.P. Woodruff).

0039-6028/02/$ - see front matter
PII: S0039-6028(01)01957-4

methods. This is particularly true in the case of quantitative structural studies, and indeed the most recent (1999) edition of the NIST *Surface Structure Database* [1] contains no entries for any molecular adsorbate on an oxide surface. Two related reasons for this dearth of experimental data have been the difficulty of preparing well-characterised single-crystal surfaces and the fact that most such bulk oxides are insulators and are thus difficult to study by incident or emitted electron methods due to the problem of charging. More recently, however, an increasing number of surface science studies have been conducted on thin epitaxial oxide films, generally overcoming the problem of surface charging and allowing in situ preparation and re-preparation [2–4]. Of course, the quality of these films is of considerable potential importance, because in some cases the surface chemistry of oxide surfaces to particular reactants can be totally dominated by the concentration of surface defects. In the case of NiO(1 0 0) films, however, grown on a variety of substrates, this does not appear to be a major problem, and the films grown on Ni(1 0 0), in particular, have been very extensively characterised by a variety of electronic, structural and chemical probes.

Recently, we showed that the technique of scanned-energy mode photoelectron diffraction (PhD) [5] could be applied to obtain the local adsorption geometry of NO adsorbed on NiO(1 0 0) grown on a Ni(1 0 0) substrate [6,7]. One conclusion of this study was that while the qualitative aspects of the structure determined experimentally were in excellent agreement with previous theoretical studies (notably that the NO bonds atop a surface Ni atoms through the N atoms with a large N–O tilt relative to the surface normal) the N–Ni nearest-neighbour distance (1.88 ± 0.02 Å) was much (≈ 0.2 Å) shorter than that found in the theoretical calculation [8,9]. In view of this it is interesting to establish similar quantitative structural information for other simple adsorbate molecules on this surface. In particular, we wish to establish whether this mismatch of current theory and experiment is unique to the case of NO adsorption, or is more general. Here we report the results of a similar study of CO and NH_3 adsorption on NiO(1 0 0) prepared in the same way. No comparable calculations exist for NH_3 adsorption on this surface, but for CO adsorption we find an even more serious discrepancy with the results of similar theoretical calculations than in the case of NO adsorption. A brief report of the main conclusions of this study have been reported elsewhere [10], but here we provide a far more complete presentation of the experimental methods, results and conclusions.

2. Experimental details

The PhD technique [5] exploits the coherent interference which occurs between the directly emitted component of the photoelectron wavefield resulting from the photoionisation of an adsorbate core level, and the components of this same wavefield which are elastically scattered by the surrounding atoms. The photoelectron kinetic energy, and thus the associated photoelectron wavelength, is varied by changing the photon energy, causing different scattering pathways to switch in and out of phase. This leads to modulations in the photoemission intensity as a function of energy in any specific direction. Using relatively low photoelectron energies (<500 eV), at which elastic backscattering cross-sections are reasonably large, these data provide quantitative information on the adsorbate–substrate registry. In the present case the C 1s PhD data from the adsorbed CO were obtained by recording a sequence of photoelectron energy distribution curves (EDCs) around the C 1s peak at 2 eV steps in photon energy in the photoelectron kinetic energy range 64–440 eV in a total of 19 different emission directions. A smaller set of 7 O 1s EDCs at 4 eV steps in the kinetic energy range 70–430 eV were also recorded although these were dominated by emission from the NiO film as discussed below. A similar N 1s data set was collected from adsorbed NH_3 on NiO(1 0 0). In our general PhD methodology these individual EDCs are fitted by the sum of a Gaussian peak, a step and a template background. The integrated areas of these peaks are then plotted as a function of photoelectron energy and the final PhD modulation spectrum obtained by sub-

traction and normalisation by a smooth spline function representing the non-diffractive intensity and instrumental factors. In the present case the individual C 1s EDCs were fitted by not just one Gaussian peak but by two chemically shifted components as described below. The necessary intense tuneable source of soft X-radiation was provided by the HE-TGM-1 monochromator [11] installed on the BESSY synchrotron radiation source in Berlin.

The experiments were conducted on a conventional ultra-high vacuum surface science end-station equipped with the usual facilities for sample cleaning, heating and cooling (including liquid helium cooling). Different electron emission directions could be detected by rotating the sample about its surface normal (to change the azimuthal angle) and about a vertical axis (to change the polar angle). Sample characterisation in situ was achieved by LEED and by soft-X-ray photoelectron spectroscopy (SXPS) using the incident synchrotron radiation. These wide-scan SXPS spectra, and the narrow-scan C 1s, N 1s and O 1s spectra used in the PhD measurements, were obtained using a VG Scientific 154 mm mean radius spherical sector electrostatic analyser equipped with three-channeltron parallel detection which was mounted at a fixed angle of 60° to the incident X-radiation in the same horizontal plane as that of the polarisation vector of the radiation.

The Ni(1 0 0) sample substrate, spark-machined from a single crystal bar after X-ray Laue alignment, was mechanically polished and subsequently cleaned in situ by cycles of argon ion bombardment and annealing, together with oxygen dosing and heating treatments to assist in the removal of surface carbon. A clean and well-ordered surface was achieved as judged by SXPS and LEED. The epitaxial NiO(1 0 0) film was grown onto this substrate by in situ oxidation, following a procedure broadly similar to that used by Kuhlenbeck et al. [8]. In particular, the sample was subjected to cycles of 1200×10^{-6} mbar s doses of oxygen at elevated temperature and higher temperature annealing. In the present case the dosing was effected while the sample cooled over a period of 60 s at a pressure of 2×10^{-5} mbar after a brief heating, leading to an estimated average dosing temperature of 370 K. The annealing temperature after each dose was 670 K. After each such cycle or sequence of cycles the surface order was checked by LEED and the O 1s to Ni 3s SXPS peak ratio checked at a photon energy of 750 eV to follow the oxygen uptake. LEED showed the first signs of the NiO(1 0 0) diffracted beams after 3 cycles, while after 8 cycles these beams were clear but coexistent with those from the Ni(1 0 0) substrate. After 13 cycles the SXPS intensity ratio appeared to saturate (at a value of 5.36) and the surface oxidation was regarded as complete. The associated LEED pattern was characteristic of the NiO(1 0 0) surface, but with rather diffuse spots as described in earlier growth characterisation studies [8]. One indication proposed to indicate a significant defect density in the case of NiO(1 0 0) films grown on Ni(1 1 0) is the appearance of a feature in the O 1s photoemission peak $\approx$1.8 eV higher in binding energy than the main peak [12]; no clearly resolved feature of this kind was evident in our data. Fig. 1 shows typical O 1s spectra recorded at a nominal photon energy of 755 eV from the clean surface and after CO adsorption; these spectra were recorded under nominal high resolution conditions, although the HE-TGM monochromator is designed for high flux rather than high resolution, so in these spectra

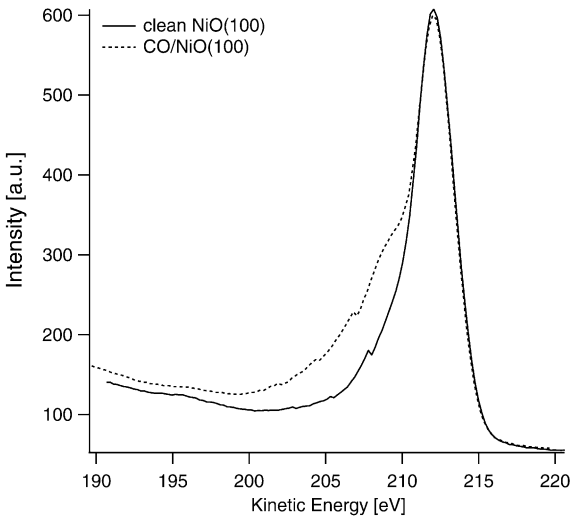

Fig. 1. Experimental 'high resolution' O 1s photoelectron energy spectra recorded from a clean NiO(1 0 0) surface and from the CO covered surface at a photon energy of 755 eV.

the total instrumental resolution is probably in excess of 2 eV. The clean surface shows an asymmetric peak with no visible shoulder, although a contribution at 1.8 eV could give rise to some of the asymmetry. The adsorbed CO clearly has an associated O 1s photoelectron binding energy which is significantly (≈5 eV) larger than that from the oxide, although it was not possible to obtain a reliable separation of these components in the (low resolution) PhD spectra to obtain useful O 1s PhD spectra from the adsorbed CO.

The issue of the degree of perfection of NiO(1 0 0) films on Ni(1 0 0) has also been investigated using spot-profile analysis LEED (SPA-LEED) and scanning tunnelling microscopy on a surface slightly miscut from (1 0 0) to yield a surface with average terrace widths between steps of ≈100 Å [13]. These authors actually concluded that the NiO film comprised small (50 Å) NiO islands which were tilted by an average angle of 8° to the (1 0 0) substrate but with a very broad distribution having a FWHM of more than 6°; the presence of these tilts was proposed to be a consequence of the large (20%) lattice mismatch. Extending this model to a nominally exact Ni(1 0 0) surface with a more random step character would imply the existence of four domains of different azimuthal orientations of the tilt angles which would lead to extremely diffuse LEED spots. We will consider the detailed consequences of this model later. These authors also concluded that some 20–25% of their NiO surface was defected. Of course, for the purposes of the present study the most significant issue concerning surface defects is to be sure that the surface defects are not so strongly active for the adsorbates of interest as to dominate the adsorption. In particular, we wish to assume, unless we have specific evidence in our data to the contrary, that the PhD data we collect from the adsorbates at essentially saturation coverage in the sub-monolayer regime are predominantly adsorbed on local sites characteristic of a defect-free surface. In this regard we should stress that temperature-programmed desorption (TPD) of CO [16] and NH_3 [14] (and NO [8,16]) from such surfaces do indicate that this is the case; indeed, in the case of NO adsorption a direct comparison of TPD from cleaved bulk NiO(1 0 0) and an epitaxial NiO(1 0 0) film shows essentially identical spectra despite the fact that the defect density on the film is believed to be orders of magnitude larger [8].

In our experiments the data from adsorbed NH_3 were obtained from a surface exposed to a nominal 5×10^{-6} mbar s of NH_3 at a sample temperature of 140 K, and then heated to ≈170 K, at which temperature the measurements were made. The slightly elevated temperature was used to ensure that no second layer adsorption occurred; such species have been reported to desorb at temperatures below 150 K [14]. CO is significantly more weakly adsorbed on NiO(1 0 0). Previous TPD studies have indicated that on both these epitaxial thin films [15,16] and on cleaved surfaces of bulk NiO [16] the first layer of adsorbed CO desorbs in the temperature range 90–150 K depending on the coverage, whereas on the cleaved surface multilayer desorption occurs around 30 K. In our experiments to study the first-layer adsorbed CO species initial attempts to work with a sample dosed with CO and then maintained at the UHV base pressure showed evidence of some time-dependent loss of adsorbate was observed, possibly due to photo-stimulated desorption. Similar but more complex incident beam related behaviour was observed in our previous study of NO adsorption on NiO(1 0 0) [6]. In order to suppress the effects of the CO desorption the PhD measurements were made during continual exposure to $\approx 4 \times 10^{-9}$ mbar of CO gas throughout the measurement time at a sample temperature of 50–80 K.

By comparing the ratio of the C 1s and N 1s photoemission intensities to the Ni substrate emission with the equivalent ratios for C 1s and O 1s to Ni for the Ni(1 1 1)(2 × 2)-CO phase with an assumed coverage of 0.5 ML [17], we can estimate the adsorbate coverages on NiO(1 0 0). The resulting values are somewhat susceptible to error due to a lack of knowledge of the relative attenuation lengths of metallic Ni and NiO (these are commonly much larger in oxides) but at high photon energies the Ni 3p and 3s emission appears to contain a large component from the underlying metal, minimising this problem. The resulting coverage estimates are 0.33 ML for CO and 0.13 ML for NH_3 with a precision of perhaps 20%.

3. Results

Our structural study is based on the analysis of the PhD data collected from the core level photoemission spectra of the adsorbed molecules. In the case of the N 1s emission from adsorbed NH_3 the spectra could be readily fitted by a single component peak and the associated PhD modulation spectra extracted in the usual way as described in the previous section. For the CO adsorption data, one would ideally aim to use separated PhD data from the C 1s and O 1s photoemission signals to give the local structural surroundings of each component atom in a largely independent fashion. For the O 1s emission, however, the dominant component of the intensity arises from the NiO substrate. As seen in Fig. 1 and discussed briefly in the previous section, we do find a significant chemical shift between the O 1s photoelectron binding energies of the oxygen atoms in the oxide and in the adsorbed CO, but separation of these components in the lower-resolution PhD EDCs failed to yield modulation spectra of value in the structural analysis. The problem is exaggerated by the very broad character of the CO-related peak in Fig. 1, which is too large to be entirely instrumental in origin, implying that it may itself comprise two or more components (as is seen for the C 1s emission, described below); the data quality and the intensity of the CO-related shoulder in the O 1s spectra are certainly inadequate to achieve a reliable and unique separation into multiple components. Attempts to separate the O 1s spectra into two components led to PhD spectra for the CO-related component which showed only weak modulations superimposed on noise of comparable size. Because the O atom in the adsorbed CO is expected to be further from the surface (if the molecule bonds through the C atom as generally expected and predicted by earlier theoretical total energy calculations [18, 19]), the O 1s PhD modulations are expected to be much weaker than those of the C 1s data. This intrinsic weakness, combined with a deterioration in the signal-to-noise ratio resulting from the peak separation, and with the possible role of two different components to this O 1s feature, conspire to render these O 1s PhD spectra of no practical value in the present structural analysis. Notice that the oxide component of the O 1s EDCs results from emission from many layers of the NiO film and so are largely characteristic of 'bulk' NiO; the PhD data which can be extracted from these components are thus of no great interest and were not analysed further.

By contrast, the C 1s data contain no contribution from substrate emission, and can be expected to show significantly stronger PhD modulations from substrate scattering. Nevertheless, there remains one complication in these data, as may be seen from a typical C 1s EDC shown in Fig. 2 which clearly has a shoulder on the high kinetic energy side indicative of two different components. These EDCs could be fitted satisfactorily using two component peaks separated by $\approx$4.5 eV as seen in Fig. 2. We assign the dominant component to adsorption at terrace sites, and the smaller component to adsorption at defect sites. Fig. 2 shows the plot of the integrated intensities of the two components as a function of photoelectron kinetic energy for normal emission. Clearly the dominant (terrace site adsorption) component shows strong PhD modulations, whereas the minority species shows only weak modulation or simply noise. The ratio of the average intensities, defined by the splines through these two curves, gives the relative contribution of the minor component as $25 \pm 5\%$, a figure compatible with estimates of defect density at the surfaces of these films obtained previously, as mentioned above. Our structure determination has thus concentrated on the analysis of the PhD modulation spectra obtained from the dominant C 1s component. The minor component showed no strong PhD modulations in any emission direction for which data were recorded, perhaps indicating that it contains contributions from several different kinds of defect-related adsorption geometries such as low-symmetry adsorption at step sites with several different step alignment directions. As remarked earlier, there was no real evidence of a similarly large defect-site component in the N 1s spectra from adsorbed NH_3. In spectra recorded at the highest available resolution there was a faint hint of a weak high-kinetic-energy component which might be attributed to defects, yet the subsequent

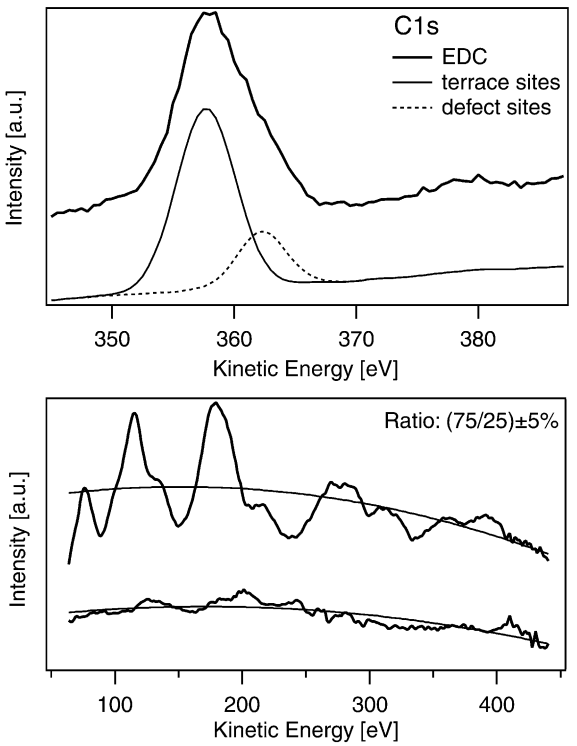

Fig. 2. C 1s photoemission data from CO adsorbed on NiO(1 0 0). The upper panel shows a single C 1s photoelectron energy distribution curve (EDC) together with the two components fitted to this spectrum; the dominant peak is attributed to emission from CO on terrace sites, while the minor component is believed to be due to CO adsorbed at defect sites. The lower panel shows the intensity of each of these components obtained by fitting many such spectra recorded at different photon energies, on the same intensity scale, as a function of kinetic energy. The smooth splines through these two curves indicate the average intensity ratio of the two components. Note the large PhD modulations of the main component and the much weaker modulations of the minor component.

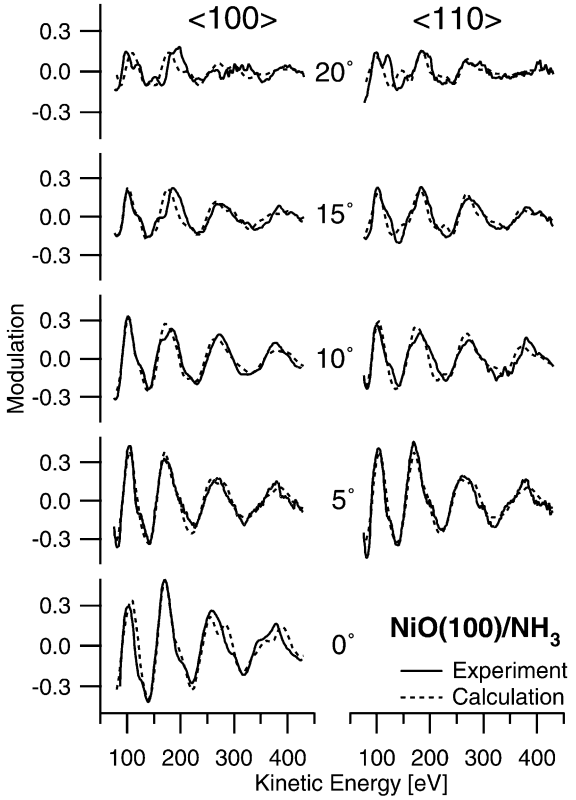

Fig. 3. Comparison of the N 1s experimental PhD modulation spectra from NH_3 adsorbed on NiO(1 0 0) with the results of the multiple scattering simulations for the best-fit structure.

PhD analysis based on the assumption that only a single component was present gave such good agreement with theory for a single terrace site that it is difficult to imagine that any defect component was significant.

The main component C 1s PhD modulation spectra from adsorbed CO, like the N 1s PhD spectra from adsorbed NH_3, typically showed quite strong modulations near normal emission to the surface, with the modulation amplitudes decreasing as the polar emission angle increased. This behaviour is rather typical of emission from an atom adsorbed in, or close to, an atop site on the surface, as we have seen in many previous examples (e.g. CO on Cu(1 1 0) [20], K [21], NH_3 [22] and PF_3 [23] on Ni(1 1 1)). Selections of 9 N 1s PhD spectra (Fig. 3) and 10 C 1s PhD spectra (Fig. 4), all of which show moderate amplitude modulations but also show this clear trend in amplitude variation, were selected for the structure analyses.

Our standard method of determining the structure from PhD data is based on a two stage process. In the first stage we apply the 'projection method' of direct data inversion [24,25] to obtain an approximate 'image' of the scattering atoms around the emitter. This method, however, like so-called holographic methods in photoelectron diffraction, only yields accurate near-neighbour information if the identity of the near-neighbour

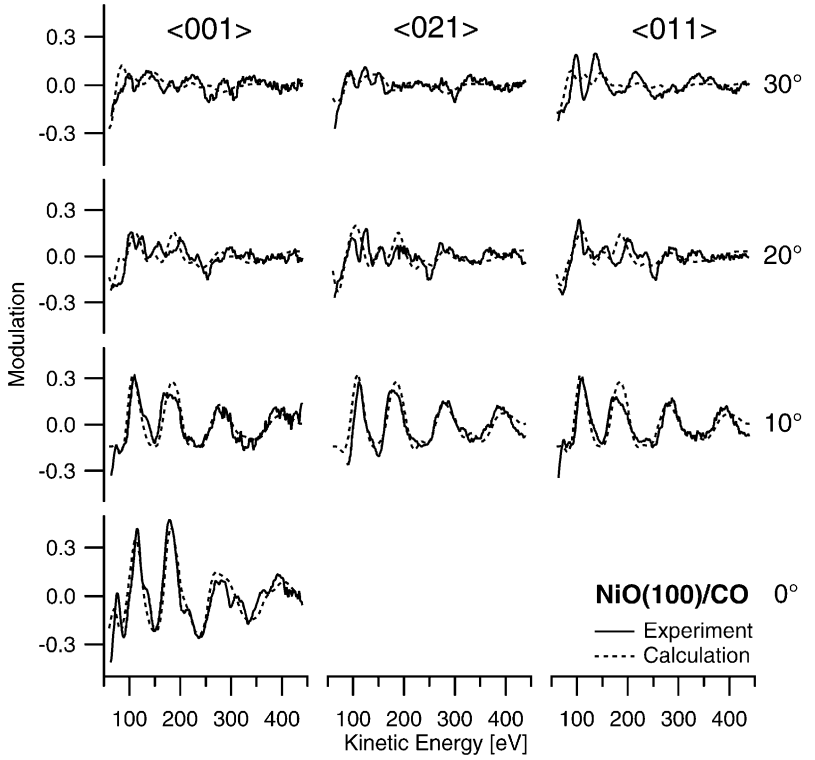

Fig. 4. Comparison of the C 1s experimental PhD modulation spectra from CO adsorbed on NiO(1 0 0) with the results of the multiple scattering simulations for the best-fit structure.

atoms is known, so that the necessary phase-shift corrections can be applied. Such a method is often very successful for an elemental substrate, but is intrinsically unsound for a compound surface [7] (and especially one comprising very different electron scattering atoms, like Ni and O). In the present case we must therefore rely entirely on what is normally the second stage of trial-and-error modelling, simulating the experimental data with multiple scattering calculations for different trial structures. These calculations are performed with codes developed by Fritzsche [26–28] which are based on the expansion of the final state wave function into a sum over all scattering pathways which the electron can take from the emitter atom to the detector outside the sample. A magnetic quantum number expansion of the free electron propagator is used to calculate the scattering contribution of an individual scattering path. Double and higher order scattering events are treated by means of the reduced angular momentum expansion (RAME). The finite energy resolution and angular acceptance of the electron energy analyser are accounted for analytically. Anisotropic vibrations for the emitter atom and isotropic vibrations for the scattering atoms are also taken into account. The comparison between theoretical and experimental modulation amplitudes, χ_{th} and χ_{ex}, is quantified by the use of a reliability factor

$$R_{\mathrm{m}} = \sum(\chi_{\mathrm{th}} - \chi_{\mathrm{ex}})^2 / \sum(\chi_{\mathrm{th}}^2 + \chi_{\mathrm{ex}}^2) \qquad (1)$$

where a value of 0 corresponds to perfect agreement, a value of 1 to uncorrelated data, and a value of 2 to anti-correlated data. The search in parameter space to locate the structure having the minimum R-factor was performed with the help of an adapted Newton–Gauss algorithm. In order to estimate the errors associated with the individual structural parameters we use an approach based

on that of Pendry which was derived for LEED [29]. This involves defining a variance in the minimum of the R-factor, R_{min} as

$$\mathrm{Var}(R_{min}) = R_{min}\sqrt{2/N} \quad (2)$$

where N is the number of 'independent pieces of structural information' contained in the set of modulation functions used in the analysis. All parameter values giving structures with R-factors less than $R_{min} + \mathrm{Var}(R_{min})$ are regarded as falling within one standard deviation of the 'best fit' structure. More details of this approach, in particular on the definition of N, can be found elsewhere [30]. In the NiO/NH_3 case here, e.g., using values of 5 eV for the imaginary part of the optical potential and of the energy broadening [30], and a total data set of nine spectra covering the range 80–430 eV we obtained a value for N of 110 and a variance of 0.012 in $R_{min} = 0.09$.

Despite our inability to use the projection method in the present study of adsorption on a compound surface, the fact that the PhD modulations are largest near normal emission for both species strongly suggests, as discussed above, that both N in NH_3 and C in CO are essentially atop surface layer atoms, and most probably atop the strong Ni scatterers in the outermost NiO(1 0 0) surface layer. In the case of CO adsorption previous theoretical (total energy) calculations for this system [18,19] favoured such a geometry in which the CO molecule bonds atop a surface Ni atom with the C closest to the surface and the C–O axis essentially perpendicular to the surface. This perpendicular orientation of CO is also supported by near-edge X-ray absorption fine structure (NEXAFS) experimental measurements [15]. In the case of the NiO(1 0 0)/NH_3 system, no such theoretical study has been reported, although we note that NH_3 is found to adsorb atop a surface Ni atom on Ni(1 1 1) [31] and Ni(1 0 0) [32]. We therefore concentrated on these basic models varying both the height and lateral offsets of the C, O and N atoms above the surface (which introduces the possibility of lower-symmetry adsorption sites and molecular tilts), and exploring possible changes in the outermost Ni nearest-neighbour layer spacing of the NiO substrate. Notice that for the NH_3 calculations the very weakly scattering H atoms were not included in the calculations. A previous attempt to use PhD data to determine the location of the H atoms in NH_3 adsorption on Cu(1 1 1) [33] led to results which were consistent with expectations, but which were far too imprecise to be of any chemical significance.

In addition to the models based on adsorption atop surface Ni atoms, multiple scattering calculations were also conducted for adsorption on O atoms in the NiO surface, and for CO adsorption through the O end in both of these sites. The results clearly favoured the expected geometries. For the NH_3 adsorption system an exceptionally low R-factor value of 0.09 was obtained for the optimised (Ni) atop geometry (see Table 1). A similar optimisation of an adsorption geometry with NH_3 atop a surface layer O atom gave a very significantly worse fit with a R-factor of 0.2. In the case of the CO adsorption data, which included the weaker PhD modulation spectra at a larger polar emission angle of 30°, the optimal geometry of CO atop Ni gave a R-factor value of 0.19, whereas the other values were: CO atop O, 0.47; OC atop Ni, 0.48; OC atop O, 0.42). These other structures can be clearly rejected as their R-factors all greatly exceed the sum of the minimum value (0.19) and the estimated variance (0.035). The optimised structures are shown schematically in Fig. 5, the associated parameter values (defined in Fig. 5) are summarised in Table 1, and the quality of the agreement between theory and experiment for the best-fit structure can be judged from the spectra of Figs. 3 and 4.

As may be seen from Table 1, the Ni–C and Ni–N distances can be determined with rather high precision because the data are concentrated in the

Table 1
Summary of the values of the structural parameters (see Fig. 5) for the best-fit adsorption geometries of CO and NH_3 on NiO(1 0 0)

Parameter	CO adsorption	NH_3 adsorption
r_{Ni-C}, r_{Ni-N}	2.07 ± 0.02 Å	2.06 ± 0.02 Å
r_{O-C}	1.15(0.10/−0.08) Å	
Δz	0.03(+0.06/−0.08) Å	0.11 ± 0.02 Å
θ_{C-O}	$12 \pm 12°$	
α_{Ni-C}, α_{Ni-N}	7(+5/−3)°	$7 \pm 6°$

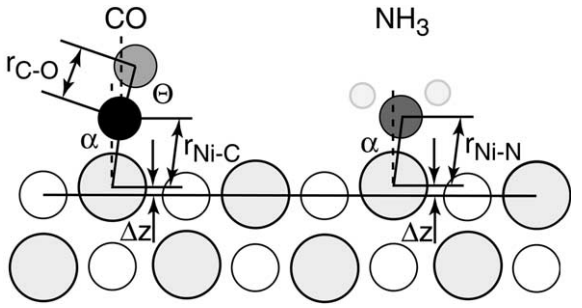

Fig. 5. Schematic side-view diagram of a NiO(1 0 0) surface showing the local geometry of the adsorbed CO and NH_3 molecules and defining the main structural parameters investigated. Note that the analysis takes no account of the H atoms in the NH_3 species. In the substrate the larger circles represent Ni atoms, the smaller circles O atoms.

geometry which ensures strong backscattering from the nearest-neighbour Ni atom relative to the C or N emitter. The C–O distance is less precise, but is consistent with the gas phase value of 1.13 Å. The tilt of the C–O molecular axis is not formally significant, while the tilts of the Ni–C and Ni–N bonds which define any offset from ideal atop geometries are only marginally significant. For this reason, there is also no significance in optimised values of the azimuthal angle of these tilts.

In addition to these static structural parameters, the fitting also involves adjustment of the mean-square vibrational amplitudes of the emitter and scatterer atoms. Our multiple scattering simulation program allows us to incorporate anisotropic vibrations parallel and perpendicular to the surface for the emitter atoms, but only isotropic vibrations for other atoms. Notice that the parameters which define the physical role of vibrations in the photoelectron diffraction process are the *relative* vibrational amplitudes of the scatterers with respect to the emitter, so the absolute values are arbitrary in the context of these calculations. In the past we have found that including the effect of anisotropic emitter vibrations is important for atop emitters if the PhD data set includes spectra at polar angles significantly removed from normal emission. This is because atop adsorbates can be expected to have very low frequency frustrated translational modes parallel to the surface, and the resultant large amplitude vibrations parallel to the surface suppresses the amplitude of electron scattering events involving a significant momentum transfer parallel to the surface. In the independent fitting of the two adsorbate systems described here, that for CO, which includes data to 30° polar emission angle, was found to benefit from including the influence of anisotropic emitter vibrations, but for the smaller angular range used in the NH_3 adsorption study, this aspect did not prove important. To simplify the fitting routine for the NH_3 data, the N emitter vibrations were therefore set to zero amplitude, and only the Ni and O substrate vibrational amplitudes optimised. To aid the comparison of the results from the two systems, the N emitters are shown with the same vibrational amplitude as that of the C atoms perpendicular to the surface, and the substrate atom emitter vibrations have been corrected for this change in assignment of the relative amplitudes to specific values for the emitter and scatterers.

As anticipated, Table 2 does show for the case of the CO that the optimum values of the emitter

Table 2
Summary of the values of the vibrational parameters used in the best-fit adsorption geometries of CO and NH_3 on NiO(1 0 0)

Parameter	CO adsorption (Å^2)	NH_3 adsorption (Å^2)
$\langle u_{C,z}\rangle^2$, $\langle u_{N,z}\rangle^2$	$(50 \pm 30)\times10^{-4}$	50×10^{-4}
$\langle u_{C,xy}\rangle^2$, $\langle u_{N,xy}\rangle^2$	$(300(+700/-300))\times10^{-4}$	50×10^{-4}
$\langle u_O\rangle^2$ (CO)	$(20(+230/-20))\times10^{-4}$	–
$\langle u_{Ni}\rangle^2$	$(50(+350/-50))\times10^{-4}$	$30\ (\pm25)\times10^{-4}$
$\langle u_O\rangle^2$ (NiO)	$>10 \times 10^{-4}$	$(60(+40/-10))\times10^{-4}$

Note that for the CO case the influence of anisotropic vibrations was included, whereas for NH_3 the absence of high polar emission angles in the PhD data set meant this effect would be suppressed. Only *relative* vibrational amplitudes with respect to the emitter are physically meaningful, so to aid comparison the N emitter vibrations have been set equal to the perpendicular vibrational amplitude of the C atoms in this table.

vibrations clearly favour large vibrational amplitudes of the C atom parallel to the surface relative to their value perpendicular to the surface. However, the precision of these values is poor, so these differences are not formally significant. Moreover, the larger number of fitting variables in this case leads to less precision than in the case of NH_3. Nevertheless, the values for the substrate vibrational amplitudes in the two cases are consistent after taking account of the estimated precision.

All of these structural models and associated calculations were based on the assumption that the NiO(1 0 0) surface lies parallel to that of the underlying Ni(1 0 0) surface. As remarked earlier, however, the results of a SPA-LEED study of the growth of NiO on a Ni surface cut very slightly off (1 0 0) lead to the conclusion that there is an angular mismatch at the Ni/NiO interfaces such that the NiO(1 0 0) surface is actually tilted by an average of 8° relative to the Ni(1 0 0) planes below. In order to understand the implications of this possibility, we have conducted further simulations of our data assuming four symmetrically equivalent rotational domains of tilted islands of this kind. The results led to an essentially identical quality of fit (for the NH_3 system there is a small but formally insignificant decrease in the *R*-factor value to 0.08) with the same values of the main structural parameters, but some slight changes of the vibrational parameters. The insensitivity of our results to the possible presence of these tilts is due to the effects of averaging over the four symmetrically equivalent domains. Notice that the model we used assumed all tilts were exactly 8°; including the broad distribution of angles seen in the SPA-LEED work would reduce our sensitivity even further. Our results therefore neither confirm nor deny this possibility of tilted oxide crystallite surfaces, but our structural conclusions are insensitive to whether or not such small tilts do occur. Checks were also conducted on the possible role of parameter coupling which may influence the estimated precision of the structural parameter values, using a Hessian matrix approach [34]. This showed some coupling of minor parameters (notably the Ni–N tilt angle to the N vibrational amplitude) but no significant effect on the key interatomic distances.

4. General discussion and conclusions

In view of the very extensive number of structural studies of CO adsorption on metal surfaces, it is surprising that this appears to be the first comparable study on an oxide surface. Very recently, however, there has been an attempt to obtain the adsorption geometry of CO on NiO(1 0 0) by performing multiple scattering simulations of the published NEXAFS spectra. The results of this investigation [35] are puzzling; the preferred geometry involves a low-symmetry off-bridging site with a C–NiO outer layer spacing of 3.1 Å corresponding to a very large Ni–C nearest-neighbour distance of more than 3.2 Å. The whole analysis is based on adjusting several parameters to match the energies of three observed spectral features and contrasts strongly with the PhD study presented here which uses a data set one to two orders of magnitude larger and is based on proven methodology.

The local adsorption geometry found in our investigation for CO is generally consistent with that found in earlier theoretical studies, and the essentially perpendicular orientation of the C–O axis is consistent with the results of the earlier NEXAFS experiments. However, the Ni–C bondlength found here is in very pronounced contrast to that favoured by the total energy calculations; the two such studies published gave values of 2.49 Å [18] and 2.86 Å [19] for this parameter, whereas our value is 2.07 Å. We should perhaps remark here that a common problem in surface diffraction experiments (certainly in LEED and PhD) is that for a relatively small experimental data range one can obtain reasonable fits of experimental intensity–energy spectra at several distinctly different layer spacings. The effect is well-documented and well-understood [36]. In order to check that a comparable quality of fit to our data could not be obtained at a much larger Ni–C distance, a search was conducted of values far larger than that corresponding to the minimum *R*-factor value quoted here. Fig. 6 shows the results in the form of a plot of the *R*-factor value as a function of Ni–C distance. Clearly the *R*-factor rises steeply for distances only slightly different from 2.07 Å, but as one approaches a value of 2.45 Å it does fall to a

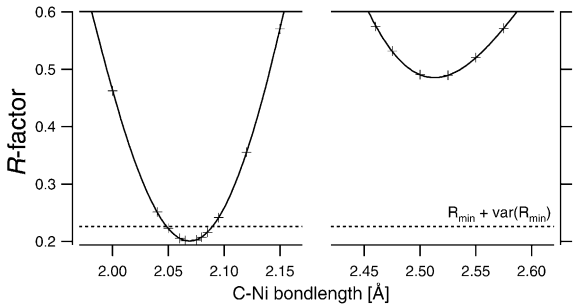

Fig. 6. Variation of the *R*-factor comparing the quality of fit between theoretically simulated and experimental C 1s PhD data from CO on NiO(1 0 0) in a Ni atop site as a function of the Ni–C nearest-neighbour distance. The dashed line corresponds to a value equalling the sum of the minimum value of the *R*-factor and its variance; all structures giving values larger than this can be formally rejected.

new local minimum (with much higher values in between). The best value of the *R*-factor at this distance, however, is 0.5, a value which exceeds that of the best-fit value by almost 9 times the estimated variance. Clearly, therefore, this large Ni–C value cannot provide a reasonable description of our data and can certainly be rejected.

While no theoretical total energy calculation exists for the NiO(1 0 0)/NH_3 system with which to compare the adsorbate bondlength, our new experimental data from this system provides us with additional information to compare the bonding of these molecular adsorbates to NiO and to metallic Ni. In Table 3 we summarise the values of the Ni-adsorbate nearest-neighbour bondlengths found in our PhD studies of CO, NO and NH_3 on NiO(1 0 0) and compare these with the theoretical values for CO and NO, and experimental values of the equivalent bondlengths for the same adsorbates on metallic Ni(1 1 1) and Ni(1 0 0). Values obtained using our PhD methodology are shown in bold; because of the uniform application of the same technique we can expect these comparisons to be particularly valid, because any systematic errors should be common. We do, however, also include some values obtained by SEXAFS, by LEED and by so-called ARPEFS (angle-resolved photoemission fine structure) which is essentially the same technique as our scanned-energy mode photoelectron diffraction although some key aspects of the methodology differ. Because bondlengths generally depend on the coordination number, we would ideally like to compare the NiO results with all the molecules in singly coordinated atop sites on metallic Ni surfaces, but the only data for NO on Ni correspond to occupation of three-fold coordinated hollow sites on Ni(1 1 1). Some insight into the influence of the change in

Table 3
Comparison of Ni–C and Ni–N nearest-neighbour distances obtained from experimental studies of CO, NO and NH_3 adsorption on NiO(1 0 0) and Ni surfaces, and of theoretical values of the same parameters for CO and NO adsorption on NiO(1 0 0)

Substrate	d_{Ni-C} (CO)/Å	d_{Ni-N} (NO)/Å	d_{Ni-N} (NH_3)/Å
NiO(1 0 0)	**2.07 ± 0.02**	**1.88 ± 0.02** [6]	**2.06 ± 0.02**
NiO(1 0 0) theory	2.49 [18], 2.86 [19]	2.1 [8]	
Ni(1 1 1)—atop	**1.77 ± 0.02** [44] (coadsorbed with O)		**1.97 ± 0.03** [31]
Ni(1 1 1)—hollow	**1.93 ± 0.03** [45]	**1.84 ± 0.07** [48]	
	1.78 ± 0.10 [46][a]	1.86 ± 0.04 [49][b]	
	1.94 ± 0.03 [47][b]	1.85 ± 0.03 [50][b]	
Ni(1 0 0)—atop	1.80 ± 0.10 [51][b]		2.01 ± 0.03 [32][c]
	1.72 ± 0.10 [52][b]		
	1.71 ± 0.10 [53][b]		
	1.70 ± 0.10 [54][b]		
	1.80 ± 0.04 [55][c]		

Values in bold face are all based on the same PhD methodology.
[a] SEXAFS.
[b] LEED.
[c] ARPEFS (PhD).

coordination number may be given by the change in Ni–C bondlength for CO adsorbed in three-fold coordinated hollow sites on Ni(1 1 1) and CO adsorbed atop on Ni(1 0 0) and on Ni(1 1 1)(2 × 2)-O discussed below.

In the case of CO adsorption, Table 3 shows that the Ni–C distance for CO in atop sites on metallic Ni surfaces is in the range 1.70–1.80 Å, roughly 0.3 Å less than on NiO(1 0 0), a very significant difference. For NH_3 the situation is less clear. On NiO(1 0 0) the Ni–N distance is 0.09 ± 0.03 Å longer than on Ni(1 1 1) obtained by the same PhD technique, but the intermediate value found in an independent study on Ni(1 0 0) indicates that the lengthening of the bond on the oxide may be marginal. For NO adsorption, the Ni–N bondlength found on NiO(1 0 0) is only slightly longer than on Ni(1 1 1), and the difference is not formally significant, bearing in mind the precision estimates. However, the Ni–C bondlength for CO adsorbed into three-fold coordinated hollow sites on Ni is very significantly longer than in atop adsorption on Ni, so if the same were to be true for NO then a similar underlying trend of bond lengthening on the oxide surface may apply.

Of course, these bondlengths should be related, albeit in a non-trivial way, to the bond strengths, so it is instructive to compare experimental estimates of the adsorption or desorption energies for these molecules on NiO and Ni. This information is provided in Table 4. For the case of CO on metallic Ni (both (1 1 1) and (1 0 0) surfaces) the values correspond to isosteric heat measurements, but in the other cases the values are based on TPD.

Table 4
Comparison of approximate adsorption/desorption energies for CO, NO and NH_3 on NiO(1 0 0) and metallic Ni surfaces, in eV per molecule

Substrate/ adsorbate	CO	NO	NH_3
Ni (experiment)	1.15–1.30 eV [56,57]	0.4 eV* [58]	0.8 eV* [59]
NiO (experiment)	0.30 eV [16]	0.57 eV [16]	0.8 eV* [14]
NiO (theory)	0.25 eV [18] 0.08 eV [19]	0.17 eV [8]	

The values marked with asterisks are crude estimates based on published TPD spectra as described in the text.

For CO and NO on NiO these involve careful analysis of the data, but the remaining values (marked with asterisks) are rather crude estimates based on the peak desorption temperatures seen in published TPD spectra; these are then fed into Redhead's standard formula assuming a value for the pre-exponential factor of 10^{13} s^{-1} [37,38]. The most striking feature of this table is the large difference in implied adsorption energy for CO on Ni and NiO; the fact that this energy is some four times larger on the metal surface, and that the value on the oxide is only 0.30 eV is clearly consistent with the large difference in Ni–C bondlength seen in Table 3. Table 4 also includes the theoretical values for CO and NO adsorption on NiO(1 0 0). In the theoretical calculations the very large Ni–C distances found are clearly consistent with the conclusions of these papers that the bonding is 'predominantly' [19] or 'almost entirely' [18] electrostatic in character, with no chemical bond formed, reflected by the very low bonding energies found in these two studies (0.08 and 0.25 eV). A similar underestimate of the bonding energy of NO in the theory for NiO(1 0 0) may be seen in Table 4. The fact that these bonding energies are too low has been recognised for some time, but the recognition that the bondlengths are also seriously in error is revealed for the first time in the present work.

One interesting feature of Table 4 is that the bonding energy of NH_3 and NO on NiO(1 0 0) is evidently *not* much weaker than on metallic Ni; indeed, the bonding of NO to NiO appears to be stronger than to metallic Ni (as reflected by peak thermal desorption temperatures of ≈220 K [16] and 140 K [58] respectively). The essentially identical peak desorption temperature for NH_3 on NiO and Ni is thus broadly consistent with the fact that the Ni–N bondlength difference in these two systems appears to be quite small; of course, the detailed character of the bonding must differ, so these values are not strictly comparable. In the case of NO the situation is less clear, because the oxide/metal comparison is for different bonding coordination; this, coupled with the anticipated difference in bonding character makes it far more difficult to draw any clear conclusions from the data.

What remains very clear, however, is that the current theoretical treatments of CO and NO bonding to NiO(1 0 0) are inadequate, leading to bonding which is much weaker than measured, and to Ni-molecule bondlengths which are very much longer than are found experimentally. Evidently, some major improvement to these theoretical treatments is required. The theoretical papers cited here are, of course, some 10 years old, but even quite recent attempts to address this problem have proved unsuccessful [9]. The general problem of achieving an accurate description of oxide/molecule bonding has been the subject of recent debates [9,39,40], but the situation is rather different for 'simple' oxides such as MgO and transition metal oxides such as NiO. In the case of MgO(1 0 0)/CO, standard local density approximation (LDA) calculations, now widely used with great success to describe bonding on metal and semiconductor surfaces, significantly underestimate the adsorption energy of this very weak adsorption system, and while stronger bonding occurs if one does not include the generalised gradient correction (GGA) [40] this 'solution' is not generally regarded as acceptable [39]. The case of NiO is rather different, because standard density functional theory methods fail to give a proper description of the electronic structure, including the band gap, and in particular do not properly describe the occupation of the Ni 3d states [41]; as such they are ill-suited to describe adsorbate bonding on the surface of the material. The approach which has therefore been regarded as more fruitful to describe NiO and adsorption at its surfaces has been to use SCF (self-consistent field) methods including various correction terms and configuration–interaction (CI). All the citations given here (included the most recent ones [9]) are based on this approach, but the resulting accuracy is evidently currently inadequate. One possible underlying problem is the use of small clusters in these calculations, which will fail to describe the electronic band properties, and may not be properly converged. In this context it is interesting to note that other SCF calculations of this type showed that CO and NO bonding strengths on NiO could be increased by using a 'weak potential', effectively lowering the ionicity [42]. To evaluate this idea effectively, however, it will be necessary to use larger clusters to eliminate the effects of the assumed charge distribution [43]. As implied above, the use of larger clusters may also bring other important benefits. Whatever the proper approach to the theory proves to be, however, the new information on adsorbate–substrate bondlengths for the molecular adsorbates on NiO(1 0 0) should prove a valuable test of such theories.

Acknowledgements

This work was supported by the German Federal Ministry of Education, Science, Research and Technology (contract no. 05 SF8EBA 4), by the Fonds der chemischen Industrie, by the European Community through Large Scale Facilities support to BESSY, and by the Physical Sciences and Engineering Research Council (UK) in the form of a research grant and a Senior Research Fellowship for DPW. DPW also acknowledges valuable discussions with Lars Petersson and Nic Harrison.

References

[1] P.R. Watson, M.A. Van Hove, K. Hermann, NIST Surface Structure Database, Ver. 3.0, NIST Standard Reference Data Program, Gaithersburg, MD, 1999.
[2] H. Kuhlenbeck, H.-J. Freund, in: D.A. King, D.P. Woodruff (Eds.), The Chemical Physics of Solid Surfaces: Growth and Properties of Ultrathin Epitaxial Layers, vol. 8, Elsevier, Amsterdam, 1997, p. 340.
[3] S.C. Street, D.W. Goodman, in: D.A. King, D.P. Woodruff (Eds.), The Chemical Physics of Solid Surfaces: Growth and Properties of Ultrathin Epitaxial Layers, vol. 8, Elsevier, Amsterdam, 1997, p. 375.
[4] D.P. Woodruff (Ed.), The Chemical Physics of Solid Surfaces: Oxide Surfaces, vol. 9, Elsevier, Amsterdam, 2001.
[5] D.P. Woodruff, A.M. Bradshaw, Rep. Prog. Phys. 57 (1994) 1029.
[6] R. Lindsay, P. Baumgartel, R. Terborg, O. Schaff, A.M. Bradshaw, D.P. Woodruff, Surf. Sci. 425 (1999) L401.
[7] M. Polcik, R. Lindsay, P. Baumgärtel, R. Terborg, O. Schaff, A.M. Bradshaw, R. Toomes, D.P. Woodruff, Faraday Disc. 114 (1999) 141.
[8] H. Kuhlenbeck, G. Odörfer, R. Jaeger, G. Illing, M. Menges, Th. Mull, H.-J. Freund, M. Pöhlchen, V. Staemmler, S. Witzel, C. Scharfschwerdt, K. Wennemann, T. Liedtke, M. Neumann, Phys. Rev. B 43 (1991) 1969.

[9] L.G.M. Pettersson, Faraday Disc. 114 (1999) 229.
[10] J.T. Hoeft, M. Kittel, M. Polcik, S. Bao, R.L. Toomes, J.-H. Kang, D.P. Woodruff, M. Pascal, C.L.A. Lamont, Phys. Rev. Lett. 87 (2001) 086101.
[11] E. Dietz, W. Braun, A.M. Bradshaw, R.L. Johnson, Nucl. Instr. Meths. A 239 (1985) 359.
[12] H. Öfner, F. Zaera, J. Phys. Chem. B 101 (1997) 9069.
[13] M. Bäumer, D. Cappus, H. Kuhlenbeck, H.-J. Freund, G. Wilhelmi, A. Brodde, H. Neddermeyer, Surf. Sci. 253 (1991) 116.
[14] M.-C. Wu, C.M. Truong, D.W. Goodman, J. Phys. Chem. 97 (1993) 4182.
[15] D. Cappus, J. Klinkmann, H. Kuhlenbeck, H.-J. Freund, Surf. Sci. 325 (1995) L421.
[16] R. Wichtendahl, M. Rodriguez-Rodrigo, U. Härtel, H. Kuhlenbeck, H.-J. Freund, Surf. Sci. 423 (1999) 90.
[17] R. Davis, D.P. Woodruff, Ph. Hofmann, O. Schaff, V. Fernandez, K.-M. Schindler, V. Fritzsche, A.M. Bradshaw, J. Phys.: Condens. Matter 8 (1996) 1367.
[18] G. Pacchioni, G. Cogliandro, P.S. Bagus, Surf. Sci. 255 (1991) 344.
[19] M. Pöhlchen, V. Staemmler, J. Chem. Phys. 97 (1992) 2583.
[20] Ph. Hofmann, K.-M. Schindler, S. Bao, V. Fritzsche, A.M. Bradshaw, D.P. Woodruff, Surf. Sci. 337 (1995) 169.
[21] R. Davis, X.-M. Hu, D.P. Woodruff, K.-U. Weiss, R. Dippel, K.-M. Schindler, Ph. Hofmann, V. Fritzsche, A.M. Bradshaw, Surf. Sci. 307–309 (1994) 632.
[22] V. Fritzsche, K.-M. Schindler, P. Gardner, A.M. Bradshaw, M.C. Asensio, D.P. Woodruff, Surf. Sci. 269/270 (1992) 35.
[23] R. Dippel, K.-U. Weiss, K.-M. Schindler, P. Gardner, V. Fritzsche, A.M. Bradshaw, M.C. Asensio, X.M. Hu, D.P. Woodruff, A.R. Gonzalez-Elipe, Chem. Phys. Lett. 199 (1992) 625.
[24] Ph. Hofmann, K.-M. Schindler, Phys. Rev. B 47 (1993) 13941.
[25] Ph. Hofmann, K.-M. Schindler, S. Bao, A.M. Bradshaw, D.P. Woodruff, Nature 368 (1994) 131.
[26] V. Fritzsche, J. Phys.: Condens. Matter 2 (1990) 1413.
[27] V. Fritzsche, Surf. Sci. 265 (1992) 187.
[28] V. Fritzsche, Surf. Sci. 213 (1989) 648.
[29] J.B. Pendry, J. Phys. C: Solid State Phys. 13 (1980) 937.
[30] N.A. Booth, R. Davis, R. Toomes, D.P. Woodruff, C. Hirschmugl, K.-M. Schindler, O. Schaff, V. Fernandez, A. Theobald, Ph. Hofmann, R. Lindsay, T. Giessel, P. Baumgärtel, A.M. Bradshaw, Surf. Sci. 387 (1997) 152.
[31] K.-M. Schindler, V. Fritzsche, M.C. Asensio, P. Gardner, D.E. Ricken, A.W. Robinson, A.M. Bradshaw, D.P. Woodruff, J.C. Conesa, A.R. González-Elipe, Phys. Rev. B 46 (1992) 4836.
[32] Y. Zheng, E. Moler, E. Hudson, Z. Hussain, D.A. Shirley, Phys. Rev. B 48 (1993) 4760.
[33] P. Baumgärtel, R. Lindsay, T. Giessel, O. Schaff, A.M. Bradshaw, D.P. Woodruff, J. Phys. Chem. B 104 (2000) 3044.
[34] R. Terborg, J.T. Hoeft, M. Polcik, R. Lindsay, O. Schaff, A.M. Bradshaw, R.L. Toomes, N.A. Booth, D.P. Woodruff, E. Rotenberg, J. Denlinger, Surf. Sci. 446 (2000) 301.
[35] F. Zhuang, J.C. Tang, J.P. He, L. Wang, Phys. Chem. Chem. Phys. 2 (2000) 3571.
[36] R. Dippel, K.-U. Weiss, K.-M. Schindler, D.P. Woodruff, P. Gardner, V. Fritzsche, A.M. Bradshaw, M.C. Asensio, Surf. Sci. 287/288 (1993) 465.
[37] P.A. Redhead, Vacuum 12 (1962) 203.
[38] See also D.P. Woodruff, T.A. Delchar, in: Modern Techniques of Surface Science, Second Edition, Cambridge University Press, Cambridge, 1994, p. 366.
[39] F. Illas, G. Pacchioni, A. Pelmenschikov, L.G.M. Pettersson, R. Dovesci, C. Pisani, K.M. Neyman, N. Rösch, Chem. Phys. Lett. 306 (1999) 202.
[40] R. Wu, Q. Zhang, Chem. Phys. Lett. 306 (1999) 205.
[41] E.g. N.M. Harrison, V.R. Saunders, R. Dovesi, W.C. Mackrodt, Phil. Trans. Roy. Soc. Lond. A 356 (1998) 75.
[42] M.A. Nygren, L.G.M. Pettersson, J. Electron. Spectrosc. Relat. Phenom. 69 (1994) 43.
[43] L.G.M. Petersson, private communication.
[44] J.-H. Kang, R.L. Toomes, J. Robinson, D.P. Woodruff, R. Terborg, M. Polcik, J.T. Hoeft, P. Baumgärtel, A.M. Bradshaw, J. Phys. Chem. B 105 (2001) 3701.
[45] M.E. Davila, M.C. Asensio, D.P. Woodruff, K.-M. Schindler, Ph. Hofmann, K.-U. Weiss, R. Dippel, P. Gardner, V. Fritzsche, A.M. Bradshaw, J.C. Conesa, A.R. González-Elipe, Surf. Sci. 311 (1994) 337.
[46] L. Becker, S. Aminpirooz, B. Hillert, M. Pedio, J. Haase, D.L. Adams, Phys. Rev. B 47 (1993) 9710.
[47] L.D. Mapledoram, M.P. Bessent, A. Wander, D.A. King, Chem. Phys. Lett. 228 (1994) 527.
[48] R. Lindsay, A. Theobald, T. Gießel, O. Schaff, A.M. Bradshaw, N.A. Booth, D.P. Woodruff, Surf. Sci. 405 (1998) L566.
[49] L.D. Mapledoram, A. Wander, D.A. King, Chem. Phys. Lett. 208 (1993) 409.
[50] N. Materer, A. Barbieri, D. Gardin, U. Starke, J.D. Batteas, M.A. Van Hove, G.A. Somorjai, Surf. Sci. 303 (1994) 319.
[51] K. Heinz, E. Lang, K. Müller, Surf. Sci. 87 (1979) 595.
[52] M. Passler, A. Ignatiev, F. Jona, D.W. Jepsen, P.M. Marcus, Phys. Rev. Lett. 43 (1979) 360.
[53] S. Andersson, J.B. Pendry, J. Phys. C: Solid State Phys. 13 (1980) 3547.
[54] S.Y. Tong, A. Maldonado, C.H. Li, M.A. Van Hove, Surf. Sci. 94 (1980) 73.
[55] S.D. Kevan, R.F. Davis, D.H. Rosenblatt, J.G. Tobin, M.G. Mason, D.A. Shirley, C.H. Li, S.Y. Tong, Phys. Rev. Lett. 46 (1981) 1629.
[56] J.C. Tracey, J. Chem. Phys. 56 (1972) 2736.
[57] K. Christmann, O. Schober, G. Ertl, J. Chem. Phys. 60 (1974) 4719.
[58] H. Conrad, G. Ertl, J. Küppers, E.E. Latta, Surf. Sci. 50 (1975) 296.
[59] C.W. Seabury, T.N. Rhodin, R.J. Purtell, R.P. Merrill, Surf. Sci. 93 (1980) 117.